Am J Cancer Res 2023;13(10):4644-4660
www.ajcr.us /ISSN:2156-6976/ajcr0151592

Original Article

Integrated analysis of EREG expression, a gene associated with cervical cancer prognosis

Shimin Yang[1*], Xu Yang[2*], Chunbo Li[1]

[1]Department of Obstetrics and Gynecology, Obstetrics and Gynecology Hospital of Fudan University, Shanghai, China; [2]Tongji Hospital of Tongji University School of Medicine, Shanghai, China. [*]Equal contributors and co-first authors.

Received June 5, 2023; Accepted August 18, 2023; Epub October 15, 2023; Published October 30, 2023

Abstract: Cervical cancer (CC) is the fourth most gynecological malignancy in the world. The identification of predictive markers can provide a basis for personalized treatment and prognostic evaluation. Our aim was to identify a new predictive marker of epiregulin (EREG) gene and explore its functional characteristics of CC and other cancer types. Differentially highly expressed genes were obtained from Gene Expression Omnibus (GEO) databases. Key genes can be verified by the Cancer Genome Atlas (TCGA) and Genotype Tissue Expression (GTEx) data, and the functions of these genes were investigated through gene ontology (GO) enrichment and Kyoto Encyclopedia of Genes and Genomes (KEGG) pathway analysis. Survival analysis were performed to determine the key genes (EREG) related to the prognosis of CC. Then, the expression difference of EREG between tumor and normal tissue was evaluated by real-time polymerase chain reaction (PCR), western blotting, and immunohistochemistry. The relationship between EREG and prognosis of patients, immune microenvironment, immune checkpoint, immune therapy and angiogenesis was discussed in 33 tumor types. Finally, the regulatory mechanism of EREG on human umbilical vein endothelial cells (HUVECs) was also explored. The differential analysis results from multiple databases showed that EREG was significantly highly expressed in CC, which was further verified in Hela and Siha cell lines. Then, Survival analysis revealed that EREG was associated with the prognosis of CC and other tumor types, and high EREG expression was significantly associated with poor prognosis. In addition, in almost all tumor types, the expression of EREG was related to immune cells infiltration, immune checkpoint genes expression and immunotherapy. Further analysis exhibited that high EREG expression can promote the high expression of angiogenesis related genes. The experimental data demonstrated that EREG could promote the proliferative, migration, invasive and tube formation of HUVECs by interacting with receptors, such as epidermal growth factor receptor (EGFR and ERBB4). EREG may be an independent prognostic marker for predicting tumor prognosis and immunotherapy response of various cancers, and may be a potential target of tumor anti-angiogenic therapy in CC.

Keywords: Pan-cancer, EREG, cervical cancer, tumor microenvironment, immune cell

Introduction

Cancer is a major public health threat worldwide, with its incidence rate and mortality increasing rapidly every year [1]. Among these cancers, CC is the fourth common gynecological malignancy [2]. Surgery and chemo-radiotherapy are considered the most effective treatment for early CC. However, treatment options for patients with recurrent or metastatic cancer are limited [3]. Long-term adverse outcomes force the exploration of new and more beneficial therapeutic strategies. Although the molecular basis of CC is complex, we need key predictive biomarkers to improve the therapeutic index and increase our understanding of drug resistance pathways to help the development of drug in future.

Epiregulin (encoded by EREG gene) is a 46-amino acid protein belonging to the epidermal growth factor (EGF) family, which is usually low expressed in most normal tissues [4]. Elevated EREG expression in various cancers mainly regulate angiogenesis and vascular remodeling and stimulate cell proliferation by binding EGFR or ERBB4 [5]. Some studies have reported that the increase of EREG levels/activity contribute to invasive growth in colorectal and gastric cancer [6, 7]. In specific cancer

types, high expression of EREG is significantly associated with short survival [8, 9]. Moreover, based on the gene expression profile of colon cancer, EREG is considered as a potential biomarker for the therapeutic effect of cetuximab [10]. Jonker et al evaluated the application of EREG as a prognostic biomarker for advanced colorectal cancer and found that high EREG expression was associated with the greater benefits of cetuximab in patients with pre-treatment and Kirsten ratsarcoma viral oncogene homolog (KRAS) wild-type colorectal cancer [11]. Interestingly, several mouse studies have shown that EREG deficiency leads to a decrease in the promotion of lung tumor, while the overexpression of EREG promotes the oncogenic feedback loop and activates the signaling pathways downstream of EGFR/ERBB4, suggesting that EREG may be a therapeutic target [12].

Although EREG has been identified as a potential prognostic biomarker for colorectal cancer, gastric cancer, head and neck squamous cell carcinoma and oral cancer [6-9, 13], there are no systematic study on the role of EREG in CC. It remains unclear whether the role of EREG may be context dependent and different in different cancers. Tumor angiogenesis is an important part of tumor progression. Previous studies have reported that EREG can contribute to the process of angiogenesis [14]. To date, few studies have explored the regulation of EREG on endothelial cells (ECs) and its potential molecular mechanism [14, 15]. For example, Sun et al reported that human esophageal cancer endothelial cells (HECEC) could enhance the invasion, migration, and metastatic potential of esophageal cancer cells through EREG [15]. In this study, we comprehensively analyzed the expression of EREG in CC and its relationship with tumor-infiltrating immune cells and related immune markers. Then, we comprehensively analyzed EREG expression and its relationship with prognosis, tumor-infiltrating immune cells and immune checkpoint gene expression and further visualized its predictive prospect in tumor immunotherapy. Finally, we explored the molecular mechanisms of EREG on HUVECs.

Methods

Data acquisition

RNA sequencing data for TCGA pan-cancer, and the Genotype Tissue Expression (GTEx) were extracted from the University of California Santa Cruz (UCSC) Xena browser (https://xena.ucsc. edu/), (https://portals.broadinstitute.org/ccle/data), and (https://gtexportal.org/home/datasets) for analysis, respectively. The entire data was filtered to remove missing and duplicated results, and the R package of "RMA" was used to covert through log2(TPM +1). In addition, the corresponding patient records were also downloaded from the UCSC browser, and the cases without follow-up records were deleted. The gene expression profiles of GSE7803, GSE9750 and GSE263514 were obtained from the comprehensive gene expression database. For GEO data, GEO2R was used for differential gene analysis (https://www.ncbi.nlm.nih.gov/geo/geo2r), while R package of "limma" was used for other differential analysis. To screen the differentially expressed genes between cancer and normal tissues, a t-test was used to analyze the expression between cancer and normal tissues. Then the genes with adjusted $P < 0.05$ and $|\log2FC| > 2$ were selected as differentially expressed genes.

Cox regression analysis and Kaplan-Meier survival

To evaluate the relationship between EREG expression and patients' prognosis, the pan-cancer samples were separated into EREG high- and low-expression groups with the medium cutoff as the cutoff value. Cox regression analysis was used to evaluate the relationship between EREG expression and overall survival (OS), disease-specific survival (DSS) and progression-free interval (PFI) with the TCGA databases. Subsequently, the Kaplan-Meier (K-M) method was used to assess the difference between EREG high- and low-expression groups, employing R packages of "survminer" and "survival". Log-rank *P*-value, hazard ratio (HR), and 95% confidence intervals were examined.

Functional and pathway enrichment analysis

After obtaining CC-related differentially expressed genes (DEGs), gene annotation enrichment analysis of GO and KEGG were performed by R package cluster profiler or metascape in order to further analyze the molecular mechanism (http://www.scape.org/) [16]. Enrichment analysis helps researchers discover novel biological functions, genotype-phenotype relationships and disease mechanisms [17].

Gene set variation analysis

Gene set variation analysis (GSVA) allows the identification of specific pathways based on transcriptomic data [18]. According to GSVA by "limma" package, each sample from the TCGA database got a score. Differential analyses were then conducted on the feature scores. The features with a log2 fold change (FC) > 0.4 (adjusted P < 0.05) were determined as significant differential expressed characteristics.

Immunological correlation analysis

The tumor immune microenvironment (TIME) mainly compose of distinct immune cell populations in tumor, which is highly associated with the antitumor immunological state in the tumor microenvironment (TME). CIBERSORT was applied to estimate the relative fractions of 22 infiltrating immune cell types in each tumor sample using R package [19]. The tumor immune dysfunction and exclusion (TIDE) (Tumor Immune Dysfunction and Exclusion (TIDE) (harvard.edu)) was exploited to infer the immunotherapic score for each sample [20]. TIDE score calculated for each tumor sample could serve as an alternative biomarker to predict response to immune checkpoint blockade. It could assess the possibility of tumor immune escape in the gene expression profile of a tumor sample. To assess the predicative value of EREG in immunotherapy, we analyzed gene expression profiles and clinical information from two large cohorts [21, 22]. All samples were categorized into high and low EREG groups based on median EREG expression. Then, the response rate of CR/PR and SD/PD was analyzed, and the survival analysis was also performed between high and low EREG groups.

Angiogenesis related genes analysis

For the aim of identifying the relevance between EREG expression and 17 angiogenesis related genes, R packages "limma", "reshape2" and "RColorBreyer" were applied to evaluate expression profile data from TCGA [23]. Visualization analysis was performed using the R package "ggplot". The correlation was significant and positive when P < 0.05 and R > 0.20.

Cell culture and reagents

Two cervical cancer cell lines (HeLa, and SiHa) and normal cervical cell line (Ect1/E6E7) obtained from the Cell Bank of Academia Sinica (Shanghai, China) were used in this study. HeLa, SiHa and Ect1/E6E7 were cultured in Roswell Park Memorial Institute (RPMI) 1640 with 10% fetal bovine serum (FBS), 100 units/ml penicillin, 100 μg/ml streptomycin and 0.025 μg/ml Amphotericin B. HUVECs were cultured in F12 supplemented with 10% FBS, 100 units/ml penicillin, 100 μg/ml streptomycin and 0.025 μg/ml Amphotericin B. All cells were cultured in a humidified atmosphere with 5% CO_2 at 37°C. An anti-glyceraldehyde-3-phosphate dehydrogenase (anti-GAPDH) antibody was obtained from Santa Cruz Biotechnology (CA, USA). Antibodies against EREG, EGFR and ERBB4 were purchased from Cell Signaling Technology (MA, USA). In this study, except for special interventions, the control group was treated in the same way as the experimental group, and the experiment was repeated at least three times.

Proliferation, migration, invasive and tube formation assays of HUVECs

Proliferation assays were performed in 96-well plates and the HUVECs culture medium was added with or without different concentrations of EREG. The medium was updated every 3 days and then the cell viability was measured by a 96-well plate reader to detect light absorbance (450 nm) at the specified time points.

Scratch assay was performed to evaluate cell migration. 1×10^5 HUVECs were inoculated on a 6-well culture plates and incubated at 37°C with 5% CO_2. After 8 hours of serum-free incubation, scratch was made with a 200 μl pipette tip. Then, HUVECs were treated in cell culture medium with or without EREG. Immediately photographed with an Olympus camera. After 12 hours of incubation, pictures were taken again with the same equipment. Image J software was used to calculate cell migration rate. The experiments were repeated three times.

The migration assay was carried out in a Transwell chamber. Cells were trypsinized, washed, and suspended with 3×10^4/24 well, Matrigel was diluted 8 folds and filled in the upper chambers, and EREG was added to the lower wells of the chambers. The plate was placed in a 37°C incubator for 24 h. After that, the cells attached to the lower surface were washed with phosphate buffer saline (PBS), fixed in 4% paraformaldehyde and stained with

5% crystal violet for 30 min. Images of the cells were captures and cell numbers were counted under a microscope with magnification of × 400.

Finally, the tube formation assays were also performed. 50 μl of ice-cold Matrigel solution (BD sciences) were added into a 96-well plate and incubated at 37°C for 30 min to solidify the gel. HUVECs were suspended in cell culture medium with or without EREG and plated at 3×10^4 cells/well. Images were captured at 2 h and 4 h, respectively. And the number of branched segments and tubular rounds were measured using Image J.

Western blotting analysis

Cells were lysed using radioimmunoprecipitation (RIPA) lysis buffer (Beyotime Biotechnology) to collect the total protein, and after that centrifuged at 4°C for 10 min. Then we would collect the supernatant and calculate the protein concentration. After being heated 95°C for 5 min, the protein samples were separated via sodium dodecyl sulfate polyacrylamide (SDS-PAGE) gel and electroblotted onto a polyvinylidene fluoride (PVDF) membrane. The membranes were blocked with 5% milk at room temperature and incubated with GAPDH, EREG, EGFR and ERBB4 overnight at 4°C. On the next day, after washing three times with TBST, then the membrane were incubated with horseradish peroxidase-conjugated (HRP-conjugated) anti-rabbit/mouse IgG for 1 h at room temperature. Immunoreactive bands were detected by the chemiluminescence system and analyzed using Image J.

Real-time PCR

According to TRIzol reagent instructions (Invitrogen), total RNA was extracted from cells and tissues. Following the guidelines of instructions, the purity and concentration of messenger RNA (mRNA) were identified, and then was reverse-transcribed into complementary deoxyribonucleic acid (cDNA). Quantitative real-time reverse transcription polymerase chain reaction (real-time PCR) using 384-well optical plates was performed with 10 μl template in a SYBR green format. The anti-GAPDH was used as endogenous control, and a 2-ΔΔCT value method was used to measure the relative expression level. The samples were tested in triplicate. Subsequently, mRNA levels were determined by real-time PCR using the following primers: EREG (F: 5'-ATCCTGGCATGTGCTAGGGT-3' and R: 5'-GTGCTCCAGAGGTCAGCCAT-3'); and GAPDH (F: 5'-TCCACCACCCTGTTGCTGTA-3' and R: 5'-ACCACAGTCCATGCCATCAC-3').

Statistical analysis

All gene expression data were normalized through a log2 transformation for the subsequent analyses [22]. R (Version 3.2.3) and Rstudio software were exploited to perform statistical analysis of the bioinformatics results. K-M method was used to assess the difference in survival between high and low EREG expression in the TCGA database. Cox regression analysis was used to evaluate the relationship between EREG expression and OS, DSS and PFI. In order to determine the relationship between risk score and pathological characteristics, Chi-square or fisher's test were used to analyze categorical variables. The correlation between two continuous variables was measured by Pearson's correlation coefficient. Quantitative data analysis was performed with the open-source software "Image J". Overall, $P < 0.05$ was considered as statistically significant.

Results

Screening results of DEGs in CC

A flowchart was graphed to describe our study in **Figure 1A**. We obtained three gene expression profiles (GSE63514, GSE9750 and GSE7803) from the GEO database. GSE7803 included 10 normal cervical samples and 24 tumor samples; GSE9750 included 24 normal cervical samples and 33 tumor samples; GSE7803 included 24 normal cervical samples and 28 tumor samples. According to the criteria (adjusted $P < 0.05$ and $|\log2FoldChange| \geq 1.5$), a venn diagram showed that 193 genes were differentially expressed in the three datasets, of which 76 were down-regulated, and 117 were up-regulated (**Figure 1B**, **1C** and Table S1). Then, we further verified the results by analyzing the differences between TCGA and GTEx. We obtained 4097 up-regulation genes and 3575 down-regulation genes. Due to a large number of DEGs, only the top 50 up-regulated and down-regulated genes with the larg-

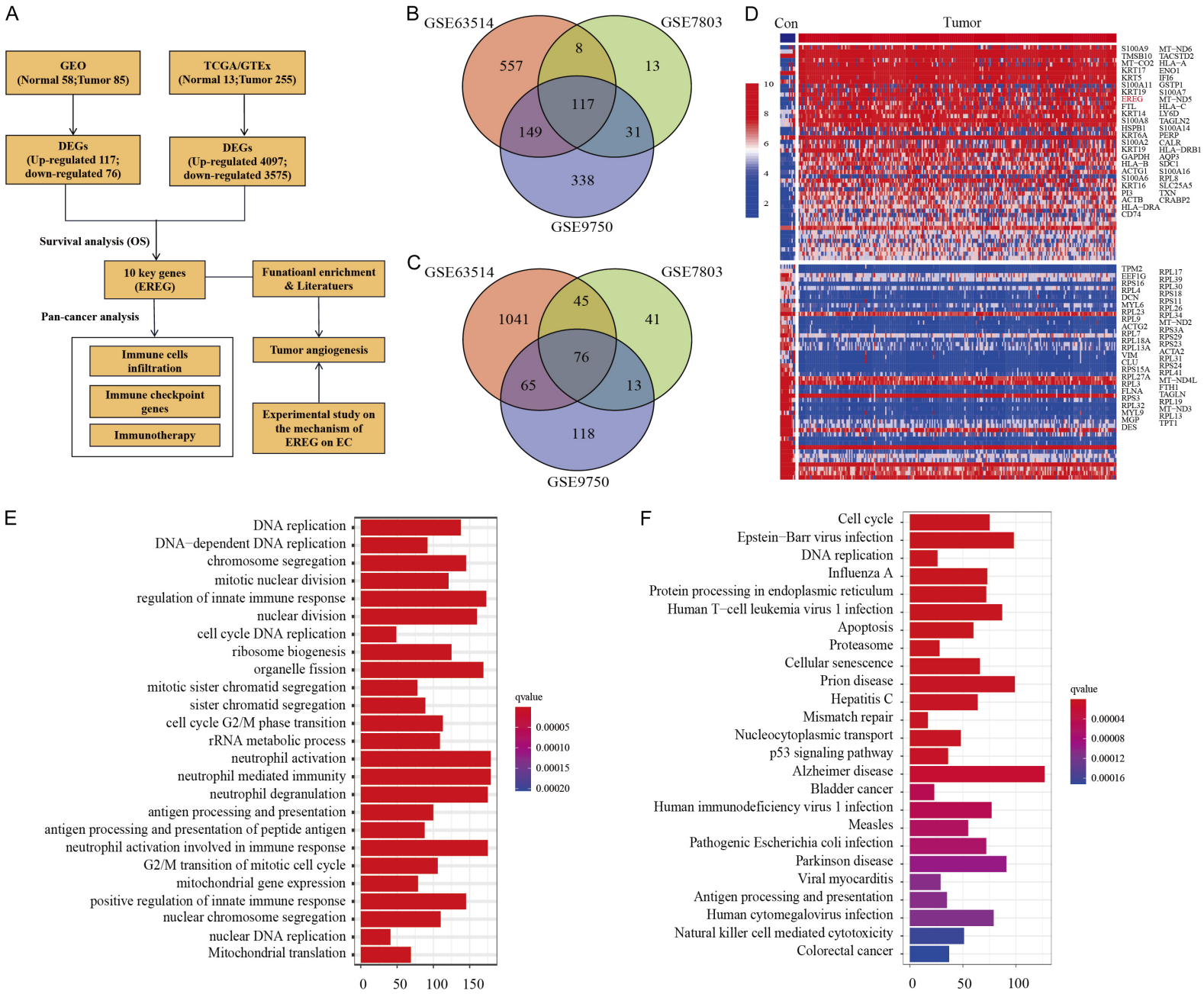
A
GEO
(Normal 58;Tumor 85)
TCGA/GTEx
(Normal 13;Tumor 255)
DEGs
(Up-regulated 117;
down-regulated 76)
DEGs
(Up-regulated 4097;
down-regulated 3575)
Survival analysis (OS)
10 key genes
(EREG)
Funatioanl enrichment
& Literatuers
Pan-cancer analysis
Immune cells
infiltration
Immune checkpoint
genes
Immunotherapy
Tumor angiogenesis
Experimental study on
the mechanism of
EREG on EC
B
GSE63514
GSE7803
GSE9750
557
8
13
117
149
31
338
C
GSE63514
GSE7803
GSE9750
1041
45
41
76
65
13
118
D
Con
Tumor
10
8
6
4
2
S100A9
TMSB10
MT−CO2
KRT17
KRT5
S100A11
KRT19
EREG
FTL
KRT14
S100A8
HSPB1
KRT6A
S100A2
KRT19
GAPDH
HLA−B
ACTG1
S100A6
KRT16
PI3
ACTB
HLA−DRA
CD74
MT−ND6
TACSTD2
HLA−A
ENO1
IFI6
GSTP1
S100A7
MT−ND5
HLA−C
LY6D
TAGLN2
S100A14
PERP
CALR
HLA−DRB1
AQP3
SDC1
S100A16
RPL8
SLC25A5
TXN
CRABP2
TPM2
EEF1G
RPS16
RPL4
DCN
MYL6
RPL23
RPL9
ACTG2
RPL7
RPL18A
RPL13A
VIM
CLU
RPS15A
RPL27A
RPL3
FLNA
RPS3
RPL32
MYL9
MGP
DES
RPL17
RPL39
RPL30
RPS18
RPS11
RPL26
RPL34
MT−ND2
RPS3A
RPS29
RPS23
ACTA2
RPL31
RPS24
RPL41
MT−ND4L
FTH1
TAGLN
RPL19
MT−ND3
RPL13
TPT1
E
DNA replication
DNA−dependent DNA replication
chromosome segregation
mitotic nuclear division
regulation of innate immune response
nuclear division
cell cycle DNA replication
ribosome biogenesis
organelle fission
mitotic sister chromatid segregation
sister chromatid segregation
cell cycle G2/M phase transition
rRNA metabolic process
neutrophil activation
neutrophil mediated immunity
neutrophil degranulation
antigen processing and presentation
antigen processing and presentation of peptide antigen
neutrophil activation involved in immune response
G2/M transition of mitotic cell cycle
mitochondrial gene expression
positive regulation of innate immune response
nuclear chromosome segregation
nuclear DNA replication
Mitochondrial translation
0
50
100
150
qvalue
0.00005
0.00010
0.00015
0.00020
F
Cell cycle
Epstein−Barr virus infection
DNA replication
Influenza A
Protein processing in endoplasmic reticulum
Human T−cell leukemia virus 1 infection
Apoptosis
Proteasome
Cellular senescence
Prion disease
Hepatitis C
Mismatch repair
Nucleocytoplasmic transport
p53 signaling pathway
Alzheimer disease
Bladder cancer
Human immunodeficiency virus 1 infection
Measles
Pathogenic Escherichia coli infection
Parkinson disease
Viral myocarditis
Antigen processing and presentation
Human cytomegalovirus infection
Natural killer cell mediated cytotoxicity
Colorectal cancer
0
50
100
qvalue
0.00004
0.00008
0.00012
0.00016

Figure 1. Schematic overview of the whole study (A); Venn diagram exhibiting the potential up-regulatory genes (B) and down-regulatory genes (C) among three GEO datasets; Heatmap plot of the top DEGs between TCGA-CESC and GTEx database (D); GO enrichment analysis (E); KEGG enrichment analysis (F).

est variations in differences were shown here as heatmaps (**Figure 1D**). Interestingly, several highly expressed genes (including EREG) screened from GEO also had high expression levels in TCGA/GTEx data. Next, GO analysis of up-regulated genes showed highly enrichment of DNA replication, chromosome segregation, neutrophil activation, neutrophil mediated immunity, antigen processing and presentation (**Figure 1E**). Similarly, KEGG pathway analysis showed highly expression of cell cycle, DNA replication, and protein processing in endoplasmic reticulum, p53 signaling pathway, antigen processing and presentation, natural killer (NK) cell medicated cytotoxicity (**Figure 1F**).

EREG is a key prognostic gene in CC and pan-cancer analysis

Cox analysis of 193 DEGs yielded 25 genes associated with the prognosis of overall survival (OS) in CC (Table S2). Then, ten key genes were obtained by crossing the 193 DEGs with 25 prognosis-associated genes (**Figure 2A**). The OS curves of these 10 genes showed the gene with the highest risk factor: EREG, which was selected for subsequent studies (**Figure 2B**). Survival analysis confirmed that high expression of EREG was associated with poor prognosis (**Figure 2C**). Then, protein-protein interaction (PPI) analysis showed that EREG, EGFR and fibroblast growth factor receptor-2 (FGFR2) were co-expressed (**Figure 2D**), indicating that EGFR and FGFR2 were two potential receptors. Further analysis indicated that EREG expression was positively correlated with EGFR, and negatively correlated with FGFR2, which was consistent with previous studies (**Figure 2E**). To further confirm the expression of EREG protein in CC, we performed immunohistochemistry in CC and normal tissue, which showed that EREG was expressed at a higher level in tumors than in normal tissues (**Figure 2F**). Then, we evaluated the mRNA and protein levels of EREG in three CC cell lines, including Hela, SiHa and Ect1/E6E7. The results showed that EREG was expressed at higher mRNA and protein in Hela and SiHa compared with Ect1/E6E7 (**Figure 2G**). These results indicated that EREG is a key prognostic gene in CC and EREG expression was closely related to the occurrence and development of CC.

In order to further reveal the value of EREG in tumors, we evaluated the expression of EREG in 33 pan-cancers. As showed in **Figure 3A**, the results showed that the EREG expression in cervical squamous cell carcinoma (CESC), colon adenocarcinoma (COAD), esophageal carcinoma (ESCA), kidney renal papillary cell carcinoma (KIRP), liver hepatocellular carcinoma (LIHC), pancreatic adenocarcinoma (PAAD), rectum adenocarcinoma (READ), stomach adenocarcinoma (STAD), thyroid carcinoma (THCA), and uterine corpus endometrial carcinoma (UCEC) was higher than that in normal tissue. Then, we analyzed the relationship between EREG expression and prognosis. Forest plots showed that in most tumor types, high EREG expression significantly affected the OS of glioblastoma multiforme (GBM), uveal melanoma (UVM), pancreatic adenocarcinoma (PAAD), kidney renal clear cell carcinoma (KIRC), CESC, adrenocortical carcinoma (ACC), brain lower grade glioma (LGG), lung squamous cell carcinoma (LUSC), THCA, bladder urothelial carcinoma (BLCA) and lung adenocarcinoma (LUAD) (**Figure 3B**). Similarly, Kaplan-Meier (KM) curves showed that EREG expression significantly affected OS of KICH, GBM, UVM, KIRC, CESC, ACC, LGG, LUSC, THCA, BLCA, and LUAD (**Figure 3C**). Meanwhile, we also explored the association between EREG expression and disease-specific survival (DSS) and progression-free interval (PFI). The results exhibited that high EREG expression was significantly correlated with DSS in LUAD, KIRP, UVM, PAAD, KIRC and CESC. KM curves showed that highly EREG expression was associated with a poor PFI in PAAD, LUSC, LUAD, LIHC, KIRC, CESC, UVM and THYM (Figure S1A, S1B). As can be seen from the above, EREG was highly expressed in tumor tissues of CC and that higher expression correlated with poor prognosis of CC patients. These results indicated that EREG may be a potential prognostic indicator in various tumor types especially for CC.

Relationship of EREG with immune cells infiltration, immune checkpoint genes and immunotherapy in CC and pan-cancer analysis

A variety of immune cells with different functions are present in the tumor microenvironment, including immunosuppressive cells and

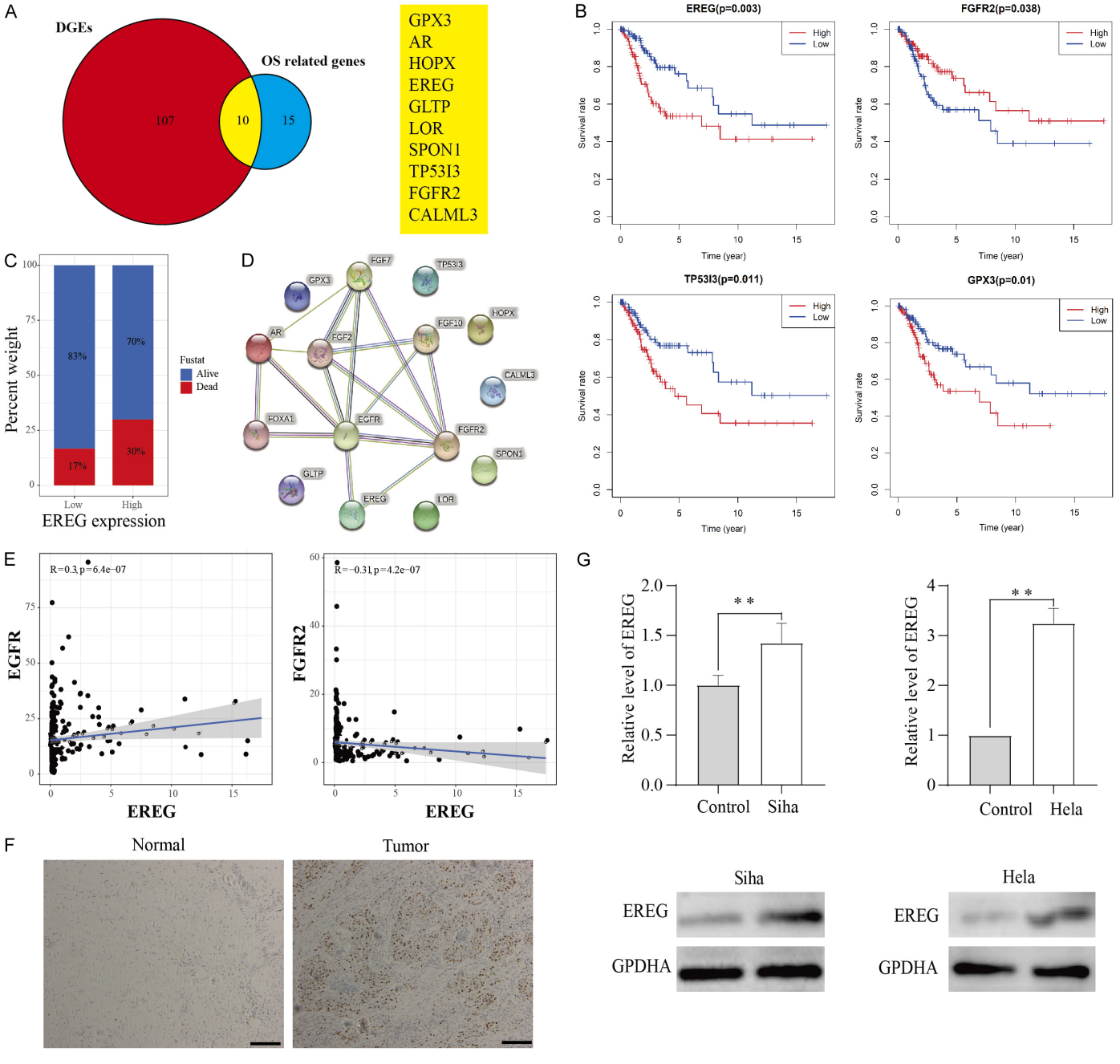
A
DGEs
OS related genes
107
10
15
GPX3
AR
HOPX
EREG
GLTP
LOR
SPON1
TP53I3
FGFR2
CALML3
B
EREG(p=0.003)
FGFR2(p=0.038)
TP53I3(p=0.011)
GPX3(p=0.01)
High
Low
Survival rate
Time (year)
C
Percent weight
83%
17%
70%
30%
Fustat
Alive
Dead
Low
High
EREG expression
D
FGF7
TP53I3
GPX3
HOPX
AR
FGF2
FGF10
CALML3
FOXA1
EGFR
FGFR2
SPON1
GLTP
EREG
LOR
E
R=0.3,p=6.4e−07
R=−0.31,p=4.2e−07
EGFR
FGFR2
EREG
G
Relative level of EREG
Control
Siha
Hela
Siha
Hela
EREG
GPDHA
F
Normal
Tumor

Figure 2. Overlap of up-regulated DEGs and prognostic genes (A); KM curves showing the 4 significantly different genes (B); The percent weight of alive and dead between high and low EREG expression (C); Construction of PPI network of 10 significant genes (D); The correlation of EREG expression with two most important receptors (EGFR and FGFR2) (E); Immunohistochemical analysis showing the difference of EREG protein between tumor and normal tissue (F); Western blotting and real-time PCR exhibiting the difference of EREG expression in Hala, Siha and let7 (control) cell lines (G).

cells that promote tumor immunity. As a result, it is necessary to continually explore the relationship between EREG and the infiltration of immune cells. The above results indicate that cervical cancer tissue has a stronger immune response (**Figure 1E**, **1F**); Therefore, we evaluated the connection of EREG expression with various immune cells in CC. The network of these cells strongly suggested overall crosstalk among all immune cells (**Figure 4A**). Further analysis showed that high EREG expression was positively correlated with activated mast cells, neutrophils and resting NK cells, while negatively correlated with M0 macrophages, resting mast cells, regulatory cells (Treg) and CD8 T cells (**Figure 4B**, **4C**). Importantly, high level of activated NK cells, activated mast cells and resting memory CD4 T cells were associated with poor prognosis (Figure S2). These results indirectly revealed the reason of high EREG with poor prognosis in CC. Immune checkpoint targeted therapy has entered the clinic for the treatment of various tumor types. We further investigated the association between EREG expression and several immune checkpoint genes. The results showed that high expression of EREG was associated with low programmed cell death 1 (PDCD1), recombinant indoleamine-2,3-dioxygenase 2 (IDO2), cytotoxic T lymphocyte associated antigen (CTLA), killer cell lectin-like receptor G1 (KLRG1), cluster of differentiation 28 (CD28), hepatitis A virus cellular receptor 2 (HAVCR2), V-set domain-containing T-cell activation inhibitor 1 (VTCN1) and T cell immunoglobulin and ITIM domain (TIGIT) expression (**Figure 4D**), which provided important evidence for EREG as a predictive biomarker for immunotherapy.

Then, we also investigated the relationship between EREG expression and immune cell infiltration in 33 tumor types. Using the median expression of EREG as the cutoff value, patients were divided into high and low expression groups. We found that high EREG expression was closely associated with high infiltration levels of resting memory CD4 T cells, activated mast cells, neutrophils and resting NK cells, while low infiltration levels of CD8 T cells, M2 macrophages, resting mast cells and activated NK cells (Figure S3A). Correlation analysis further proved the conclusion (Figure S3B). Further analysis indicated that patients with high infiltration levels of CD8 T cell, naive CD4 T cells, Treg, activated NK cells, resting dendritic cells, resting mast cells and naive B cells had better prognosis (Figure S3C). In addition, we also evaluated the connection of EREG expression with immune cells in various tumor types, respectively. The results showed that high EREG expression was negatively correlated with the infiltration levels of CD8 T cells, activated NK cells, resting mast cells in almost all tumors (Figure S3D). Finally, we collected common immune checkpoint genes (B and T lymphocyte attenuator (BTLA), CD274, TIGIT, PDCD1, HAVCR2, CTLA4 and lymphocyte activation gene-3 (LAG3)) to analyze the relationship between EREG expression and immune checkpoint genes in pan-cancer. The results showed that the expression of EREG was negatively correlated with the expression levels of immune checkpoint genes in various types of tumors (Figure S3E), which further demonstrated the value of EREG in predicating the effect of immunotherapy.

Since EREG expression was highly associated with the prognosis and immune infiltration density of CC and pan-cancer, we then tested whether EREG expression could predict the immunotherapeutic response of immune checkpoint inhibitors (ICIs). The TIDE web program was used to infer the immunotherapy response of TCGA-CESC patients. We excitedly found that the response rate of patients with high EREG expression was higher than that of patients with low TIDE score (Chi-square test, $P < 0.01$) and immune exclusion score (Chi-square test, $P < 0.01$) (**Figure 4E**). To further validate the predictive ability of EREG expression in immunotherapy, we analyzed two studies that evaluated the association of EREG expression with clinical response and prognosis to immunotherapy. In the cohort of Braun et al [20], the low EREG group was associated

EREG expression with cervical cancer prognosis

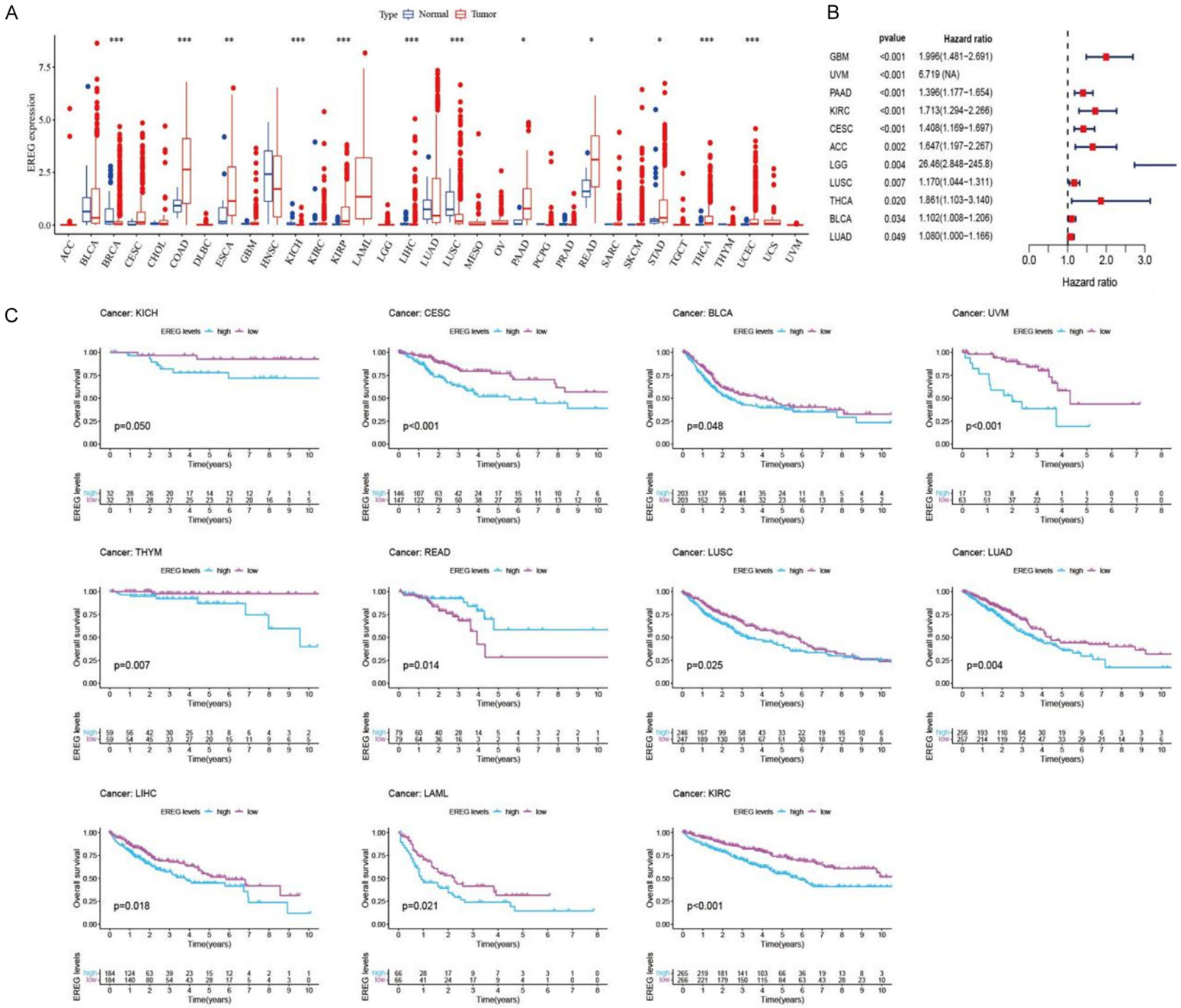

Figure 3. The difference of EREG expression between tumor and normal tissue in 33 tumor types (A); Forest plot showing the relationship between EREG expression and OS in 11 cancers with statistical differences (B); KM curves of high and low EREG expression in 11 tumors with OS survival (C).

with a better clinical response to immunotherapy (chi-square test, $P < 0.05$) (Figure S4A). Survival analysis exhibited that patients with high LMS score had prognosis prognosis than those with low LMS score (log-rank test, P=0.048) (Figure S4B). In the IMvigor210 cohort [21], the proportion of responders (CR/PR) was higher in the low EREG group than in high EREG group (chi-square test, $P < 0.05$) (Figure S4C). Survival analysis also confirmed that patients with low EREG expression had better prognosis than those with high EREG group (log-rank test, P=0.031) (Figure S4D). These results further demonstrated that patients with high EREG expression had poor response for immunotherapy, and EREG could be used as a marker for predicting the effect of immunotherpy.

High EREG was associated with angiogenesis related signaling pathway

Several studies have reported notable connections of EREG expression with endothelial cells (ECs) and angiogenesis-related signaling pathway [14, 15]. Based on pan-cancer data, GSVA revealed that EREG expression was involved in the regulation of many cancer metabolism and cancer immune signaling pathways (**Figure 5A**). High EREG expression was correlated to notable metabolism-related pathways such as tricarboxylic acid cycle (TCA), peroxisome, fatty acid metabolism and oxidative phosphorylation. These results indicated that tumor cells with high EREG expression had high metabolic capacity. Then, we explored the association of EREG expression with angiogenesis related signaling pathways, including the transforming growth factor-β (TGF-β), fibroblast growth factor/fibroblast growth factor receptor (FGF/FGFR), platelet-derived growth factor/platelet-derived growth factor receptor (PDGF/PDGFR), and hepatocyte growth factor/hepatocyte growth factor receptor (HGF/MET) signaling pathways. We found that high EREG expression was closely associated with almost all angiogenesis-related genes in most tumor types (**Figure 5B**), indicating that EREG did promote tumor angiogenesis.

Regulation of EREG on ECs by EGFR and ERBB4 receptors

In order to evaluate the effect of EREG on ECs, we firstly evaluated the association of EREG expression with VEGF and TGF-β/smad signaling pathway between high and low-expression of EREG in 33 tumor types. The activation of TGF-β/smad signaling pathway could inhibit the immune function and promote the proliferation of tumor cells. Violin figure exhibited that high expression of EREG was associated with high enrichment level of vascular endothelial growth factor (VEGF) and TGF-β/smad signaling pathway ($P < 0.01$) (**Figure 6A**, **6B**). These outcomes indicated that EREG expression was associated with tumor angiogenesis. To verify the theory, we evaluated the effect of EREG on ECs. Scratch test confirmed that EREG can promote the migration of ECs and the effect increased with the increase of EREG concentration (**Figure 6C**). Statistical analysis showed that the promotion effect was the largest when the concentration of EREG was 10 ng/ml (**Figure 6D**). Meanwhile, cell counting kit-8 (CCK8) test and invasive assay exhibited that EREG could promote the proliferation and migration of ECs. When the concentration of EREG was 10 ng/ml, the effect reached the peak (**Figure 6E**, **6F**). Overall, our data revealed that EREG could affect EC proliferative, migration and invasion of ECs. Finally, we evaluated the effect of EREG on angiogenesis. Tube formation experiments showed that high concentrations of EREG could shape better angiogenesis than low-concentration of EREG (**Figure 6G**, **6H**). It is reported that EREG is a relatively widely receptor binding ligand, which can directly activate EGFR and ERBB4 homodimers, and activate downstream signaling pathway. Our results showed that EREG could promote the high expression level of EGFR protein and mRNA. With the increase of EREG concentration, the expression level gradually increased (**Figure 6I**, **6J**). It is reported that EREG-EGFR pathway is the key axis driving tumorigenesis, and eriotinib is an important EGFR inhibitor. As shown in Figure S5A, S5B, the effect of EREG on ECs could be attenuated by eriotinib. Taken together, these data sug-

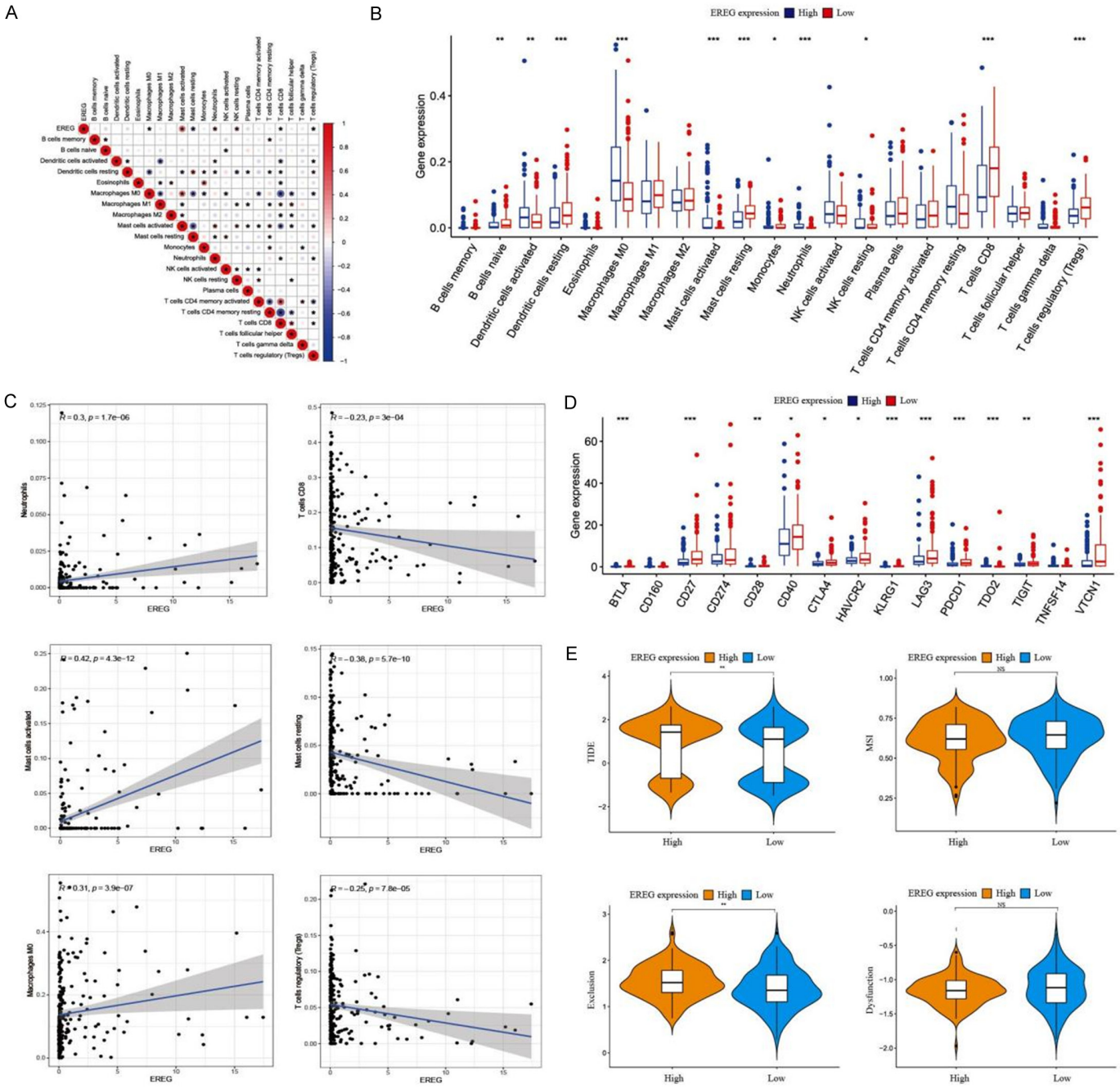
A
B
EREG expression High Low
Gene expression
B cells memory
B cells naive
Dendritic cells activated
Dendritic cells resting
Eosinophils
Macrophages M0
Macrophages M1
Macrophages M2
Mast cells activated
Mast cells resting
Monocytes
Neutrophils
NK cells activated
NK cells resting
Plasma cells
T cells CD4 memory activated
T cells CD4 memory resting
T cells CD8
T cells follicular helper
T cells gamma delta
T cells regulatory (Tregs)
C
R = 0.3, p = 1.7e−06
R = −0.23, p = 3e−04
R = 0.42, p = 4.3e−12
R = −0.38, p = 5.7e−10
R = 0.31, p = 3.9e−07
R = −0.25, p = 7.8e−05
EREG
D
BTLA
CD160
CD27
CD274
CD28
CD40
CTLA4
HAVCR2
KLRG1
LAG3
PDCD1
TDO2
TIGIT
TNFSF14
VTCN1
E
TIDE
MSI
Exclusion
Dysfunction
High
Low
NS

Figure 4. Cellular interaction of immune cells with EREG in TME in CC (A); Immune infiltration level between high- and low EREG expression (B); The correlation of EREG expression with neutrophils, CD8 T cells, resting mast cells, activated mast cells, M0 macrophages and Treg (C); The difference of immune checkpoint genes between high- and low EREG expression (D); The difference of TIDE, MSI, immune exclusion and immune dysfunction between high- and low EREG expression (E). (*P < 0.05; **P < 0.01; ***P < 0.001).

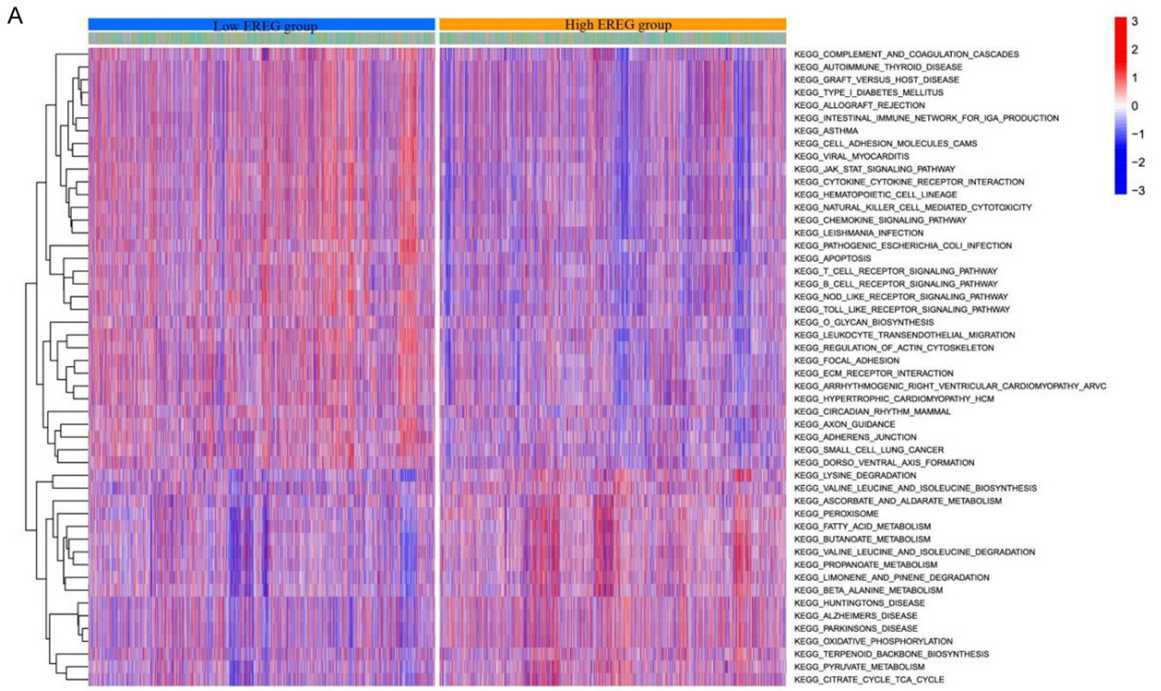

Figure 5. Pheatmap showing the enrichment difference of EREG expression in pan-cancer analysis (A); The co-expression analysis between EREG and tumor angiogenesis related genes in 33 tumor types (B). (*P < 0.05; **P < 0.01; ***P < 0.001).

gested that EREG could promote angiogenesis by inducing EGFR and ERBB4 expression.

Discussion

Various studies have revealed that EREG is highly expressed in most cancer tissues and plays a key role in cancer progression, thus conferring malignant tumor phenotype [5]. Although EREG plays an important role in regulating various cellular functions in human cancers, the oncogenic effect of EREG in CC has not been thoroughly investigated. In this study, we found that the expression of EREG in CC tis-

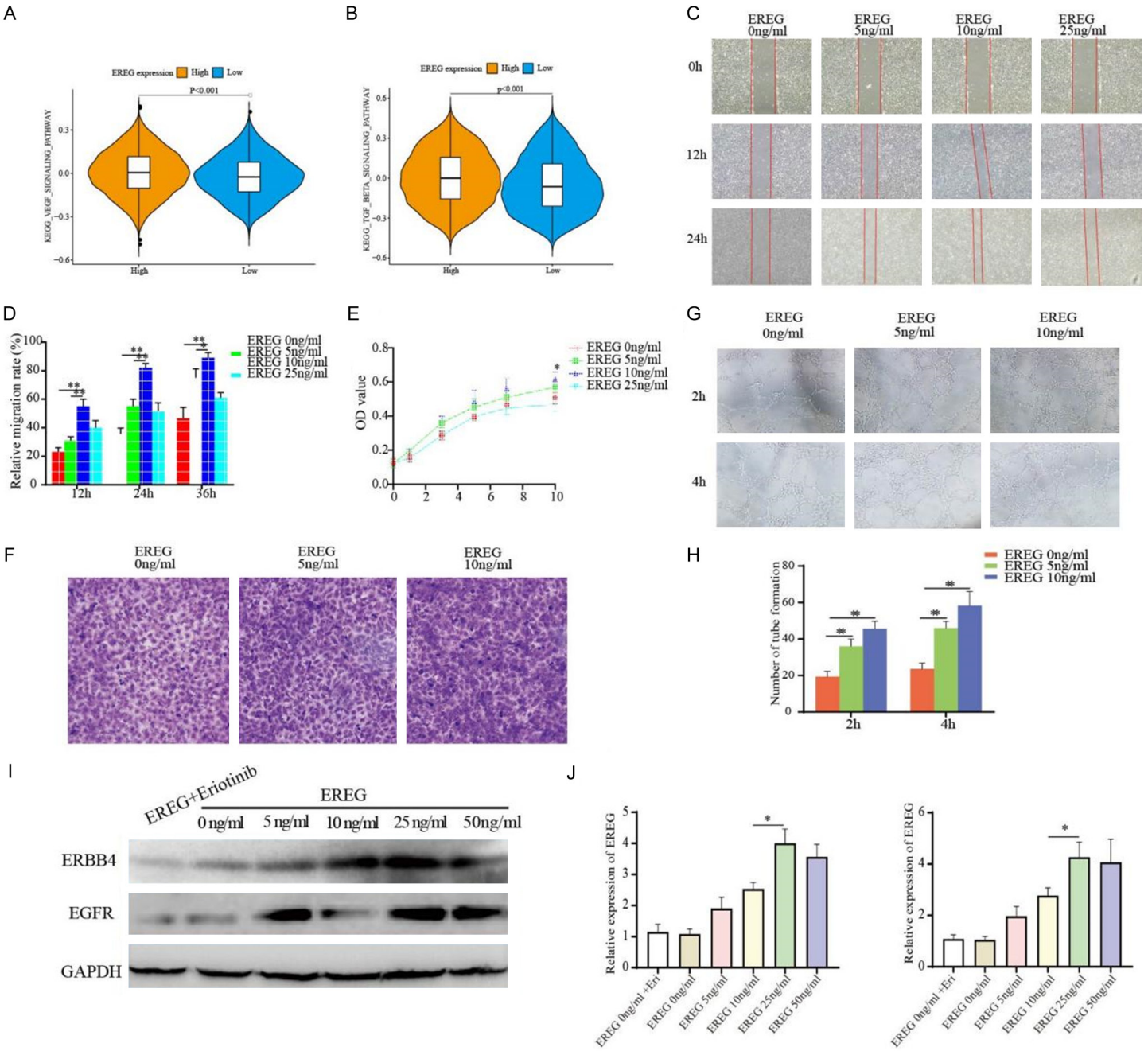
A
EREG expression High Low
P<0.001
KEGG_VEGF_SIGNALING_PATHWAY
High
Low
B
EREG expression High Low
p<0.001
KEGG_TGF_BETA_SIGNALING_PATHWAY
High
Low
C
EREG 0ng/ml
EREG 5ng/ml
EREG 10ng/ml
EREG 25ng/ml
0h
12h
24h
D
Relative migration rate (%)
EREG 0ng/ml
EREG 5ng/ml
EREG 10ng/ml
EREG 25ng/ml
12h
24h
36h
E
OD value
EREG 0ng/ml
EREG 5ng/ml
EREG 10ng/ml
EREG 25ng/ml
G
EREG 0ng/ml
EREG 5ng/ml
EREG 10ng/ml
2h
4h
F
EREG 0ng/ml
EREG 5ng/ml
EREG 10ng/ml
H
Number of tube formation
EREG 0ng/ml
EREG 5ng/ml
EREG 10ng/ml
2h
4h
I
EREG+Eriotinib
EREG
0 ng/ml
5 ng/ml
10 ng/ml
25 ng/ml
50ng/ml
ERBB4
EGFR
GAPDH
J
Relative expression of EREG
EREG 0ng/ml +Eri
EREG 0ng/ml
EREG 5ng/ml
EREG 10ng/ml
EREG 25ng/ml
EREG 50ng/ml
Relative expression of EREG
EREG 0ng/ml +Eri
EREG 0ng/ml
EREG 5ng/ml
EREG 10ng/ml
EREG 25ng/ml
EREG 50ng/ml

Figure 6. Violin figure showing the enrichment difference of VEGF signaling pathway between high- and low EREG expression in CC (*P < 0.05; **P < 0.01; ***P < 0.001) (A); Violin figure showing the enrichment difference of TGF-β signaling pathway between high- and low EREG expression in CC (B); Scratch test showing the effect of different dose of EREG on ECs migration (C); Statistical analysis exhibiting the migration rate of cells among different EREG dose (D); CCK8 showing the effect of different dose EREG on cell proliferative (E); Transwell assays exhibiting the effect of EREG on ECs invasive (F); Tube formation test evaluating the effect of EREG on ECs tubule forming ability (G, H); Western blotting and real-time PCR exhibiting the effect of EREG on ERBB4 and EGFR protein and mRNA, respectively (I, J). (*P < 0.05; **P < 0.01; ***P < 0.001).

sue was higher than that in normal tissue and demonstrated that high EREG expression was associated with poor prognosis of CC. In pan-tumor analysis, EREG expression was related to immune cell infiltration, immune checkpoint genes, and immunotherapy. Finally, we found that EREG could regulate the function of ECs and might be a potential therapeutic target of CC.

EREG is initially expressed as a transmembrane precursor and then released from the extracellular region as a mature soluble factor [24]. EREG has been detected in a variety of human cancers, including colon cancer, oral squamous epithelial cell carcinoma, lung carcinoma, bladder cancer, breast cancer, liver cancer, ovarian cancer, thyroid cancer, and malignant fibrous histiocytoma [25]. However, EREG expression is extremely low in normal tissues corresponding to tumor tissues. In this study, we found that the expression level of EREG mRNA in CC was higher than that in normal tissue according to TCGA and GEO datasets. Importantly, in vitro experiment, we used immunohistochemistry to detect the high expression of EREG protein in CC. Real-time PCR showed that compared with normal cells, the expression of EREG mRNA in Hela and SiHa was higher. This result is in accordance with previous reports on oral squamous epithelial cell carcinoma and gastric cancer [26-29]. In pan-cancer analysis, the expression level of EREG in COAD, ESCA, KIRP, LIHC, PAAD, and READ tissue was higher than that in normal tissues. Then, we evaluated the relationship between EREG expression and the prognosis of various tumor types. The outcomes showed that the high expression of EREG was related to poor prognosis in a variety of tumor types; therefor, EREG may be a potential prognostic factor [30, 31].

Increasing numbers of studies have shown that tumor immune infiltrating cells are closely related to the effect of immune checkpoint inhibition [32, 33]. In order to clarify the relationship between EREG expression and prognosis, we first examined the relative proportion of infiltrating immune cells. In CC, increased EREG expression was markedly associated with higher levels of immune cell infiltration, such as neutrophils, activated mast cells, macrophages M0 and resting NK cells, but negatively correction with CD8+ T cells, resting mast cells and regulatory T cells. Similarly, in pan-cancer analysis, we found that EREG expression was widely associated with immune cells infiltration in most tumor types. Currently, the presence of CD8 T cells in epithelial tumors is a well-supported marker of better prognosis in many tumor types [34, 35]. Meanwhile, the infiltration of mast cells may play a key role in the early stage of innate immune response to pathogens [32]. Our study demonstrated that high infiltration levels of resting mast cells and CD8+ T cells were correlated to better prognosis, which is consistent with the EREG signature in CC. Meanwhile, the expression of immune checkpoint genes in low EREG expression group was significantly increased, including BTLA, CD27, LAG3, CTLA4, PDCD1, and TIGIT. These data provide important evidence for EREG as a predictive biomarker for CC immunotherapy.

Tumor angiogenesis is a process of forming new blood vessels from existing blood vessels, which leads to a variety of diseases [36]. It is believed that it is mainly caused by the secretion of vascular endothelial growth factor-A (VEGF-A) in a variety of tumors [37]. Anti-angiogenic therapy for solid tumors is effective in the treatment of cancer patients [38]. In order to further explore the potential molecular mechanism of EREG on tumor angiogenesis, we evaluated the effect of EREG on ECs. Our results showed that EREG can promote proliferation, migration, invasive and tube formation of ECs, suggesting that EREG may result in angiogenesis during tumor progression. In addition, we also found that high EREG expression was correlated to the high enrichment of

angiogenesis related pathways, such as VEGF, FGF, PDGF, and/or other angiogenesis signaling pathways. The positive correlation between EREG expression and tumor angiogenic genes suggests indicates that EREG can promote tumor angiogenesis, which especially explained the reason why the high expression of EREG had poor prognosis. Thus, EREG can be considered as a novel target for tumor anti-angiogenenic therapy. Cetuximab, an anti-EGFR monoclonal antibody, has shown efficacy in several epithelial tumors [39]. In particular, cetuximab combined with chemotherapy can prolong the survival of patients with advanced colorectal and head and neck cancer compared with chemotherapy alone [40]. However, some studies reported that cetuximab combined with carboplatin and paclitaxel did not improve the prognosis in patients with advanced or recurrent CC [41-44]. Thus, we proposed that the combination anti-angiogenic therapy and targeted therapy (anti-EGFR monoclonal antibody) may improve the prognosis of advanced or recurrent CC.

Even though the functional role of EREG in CC and pan-cancer was explored and analyzed, and the results are of clinical significance, there were still some limitations in the current study. Bioinformatics methods used for gene identification lacks novelty to identify the prognostic signature, more grouped variable selection methods should be used. Although our experiments confirmed some conclusions, more in vitro or in vivo biological experiments are needed to validate our findings and facilitate clinical applications. Further mechanistic studies will be beneficial for elucidating the role of EREG at the molecular and cellular levels. Furthermore, despite the finding that EREG expression was correlated with tumor angiogenesis, we were not sure that whether other signaling pathways are also involved in the regulatory process.

In conclusion, our study exhibited that EREG is highly expressed in CC tissue and is associated with immune cells infiltration. It can be used as a predictor of immunotherapeutic effect and CC prognosis. Since EREG is closely related to the upregulation of tumor angiogenesis related pathways, EREG may be considered as a novel target for anti-angiogenesis therapy. Future prospective studies will focus on the regulatory function of EREG in tumor immune microenvironment and angiogenesis, which may help to improve anti-cancer strategies based on immunity and angiogenesis.

Acknowledgements

This study was supported by the Shanghai Municipal Health Commission (20194Y0085) to CB Li, and the Shanghai "Rising Stars of Medical Talent" Youth Development Program (SHWSRS2020087) to CB Li.

Disclosure of conflict of interest

None.

Address correspondence to: Dr. Chunbo Li, Department of Obstetrics and Gynecology, Obstetrics and Gynecology Hospital of Fudan University, 419 Fangxie Road, Shanghai 200011, China. Tel: +86-33189900; Fax: +86-21-63455090; E-mail: lichunbo142@126.com

References

[1] Bray F, Ferlay J, Soerjomataram I, Siegel RL, Torre LA and Jemal A. Global cancer statistics 2018: GLOBOCAN estimates of incidence and mortality worldwide for 36 cancers in 185 countries. CA Cancer J Clin 2018; 68: 394-424.

[2] Vu M, Yu J, Awolude OA and Chuang L. Cervical cancer worldwide. Curr Probl Cancer 2018; 42: 457-465.

[3] Hill EK. Updates in cervical cancer treatment. Clin Obstet Gynecol 2020; 63: 3-11.

[4] Toyoda H, Komurasaki T, Uchida D, Takayama Y, Isobe T, Okuyama T and Hanada K. Epiregulin. A novel epidermal growth factor with mitogenic activity for rat primary hepatocytes. J Biol Chem 1995; 270: 7495-500.

[5] Riese DJ 2nd and Cullum RL. Epiregulin: roles in normal physiology and cancer. Semin Cell Dev Biol 2014; 28: 49-56.

[6] Yang J, Li S, Wang B, Wu Y, Chen Z, Lv M, Lin Y and Yang J. Potential biomarkers for anti-EGFR therapy in metastatic colorectal cancer. Tumour Biol 2016; 37: 11645-11655.

[7] Xia Q, Zhou Y, Yong H, Wang X, Zhao W, Ding G, Zhu J, Li X, Feng Z and Wang B. Elevated epiregulin expression predicts poor prognosis in gastric cancer. Pathol Res Pract 2019; 215: 873-879.

[8] Sunaga N and Kaira K. Epiregulin as a therapeutic target in non-small-cell lung cancer. Lung Cancer (Auckl) 2015; 6: 91-98.

[9] Kohsaka S, Hinohara K, Wang L, Nishimura T, Urushido M, Yachi K, Tsuda M, Tanino M, Kimu-

ra T, Nishihara H, Gotoh N and Tanaka S. Epiregulin enhances tumorigenicity by activating the ERK/MAPK pathway in glioblastoma. Neuro Oncol 2014; 16: 960-70.
[10] Job S, Reyniès A, Heller B, Weiss A, Guérin E, Macabre C, Ledrappier S, Bour C, Wasylyk C, Etienne-Selloum N, Brino L, Gaiddon C, Wasylyk B and Jung AC. Preferential response of basal-Like head and neck squamous cell carcinoma cell lines to EGFR-targeted therapy depending on EREG-driven oncogenic addiction. Cancers (Basel) 2019; 11: 795.
[11] Jonker DJ, Karapetis CS, Harbison C, O'Callaghan CJ, Tu D, Simes RJ, Malone DP, Langer C, Tebbutt N, Price TJ, Shapiro J, Siu LL, Wong RP, Bjarnason G, Moore MJ, Zalcberg JR and Khambata-Ford S. Epiregulin gene expression as a biomarker of benefit from cetuximab in the treatment of advanced colorectal cancer. Br J Cancer 2014; 110: 648-55.
[12] Zhang J, Iwanaga K, Choi KC, Wislez M, Raso MG, Wei W, Wistuba II and Kurie JM. Intratumoral epiregulin is a marker of advanced disease in non-small cell lung cancer patients and confers invasive properties on EGFR-mutant cells. Cancer Prev Res (Phila) 2008; 1: 201-7.
[13] Liu S, Wang Y, Han Y, Xia W, Zhang L, Xu S, Ju H, Zhang X, Ren G, Liu L, Ye W, Zhang Z and Hu J. EREG-driven oncogenesis of head and neck squamous cell carcinoma exhibits higher sensitivity to erlotinib therapy. Theranostics 2020; 10: 10589-10605.
[14] Yang WW, Yang LQ, Zhao F, Chen CW, Xu LH, Fu J, Li SL and Ge XY. Epiregulin promotes lung metastasis of salivary adenoid cystic carcinoma. Theranostics 2017; 7: 3700-3714.
[15] Sun L, Pan J, Yu L, Liu H, Shu X, Sun L, Lou J, Yang Z and Ran Y. Tumor endothelial cells promote metastasis and cancer stem cell-like phenotype through elevated Epiregulin in esophageal cancer. Am J Cancer Res 2016; 6: 2277-2288.
[16] Zhou Y, Zhou B, Pache L, Chang M, Khodabakhshi AH, Tanaseichuk O, Benner C and Chanda SK. Metascape provides a biologist-oriented resource for the analysis of systems-level datasets. Nat Commun 2019; 10: 1523.
[17] Pan T, Wang S and Wang Z. An integrated analysis identified TAGLN2 As an oncogene indicator related to prognosis and immunity in pan-cancer. J Cancer 2023; 14: 1809-1836.
[18] Hänzelmann S, Castelo R and Guinney J. GSVA: gene set variation analysis for microarray and RNA-seq data. BMC Bioinformatics 2013; 14: 7.
[19] Yoshihara K, Shahmoradgoli M, Martínez E, Vegesna R, Kim H, Torres-Garcia W, Treviño V, Shen H, Laird PW, Levine DA, Carter SL, Getz G, Stemke-Hale K, Mills GB and Verhaak RG. Inferring tumour purity and stromal and immune cell admixture from expression data. Nat Commun 2013; 4: 2612.
[20] Jiang P, Gu S, Pan D, Fu J, Sahu A, Hu X, Li Z, Traugh N, Bu X, Li B, Liu J, Freeman GJ, Brown MA, Wucherpfennig KW and Liu XS. Signatures of T cell dysfunction and exclusion predict cancer immunotherapy response. Nat Med 2018; 24: 1550-1558.
[21] Braun DA, Hou Y, Bakouny Z, Ficial M, Sant' Angelo M, Forman J, Ross-Macdonald P, Berger AC, Jegede OA, Elagina L, Steinharter J, Sun M, Wind-Rotolo M, Pignon JC, Cherniack AD, Lichtenstein L, Neuberg D, Catalano P, Freeman GJ, Sharpe AH, McDermott DF, Van Allen EM, Signoretti S, Wu CJ, Shukla SA and Choueiri TK. Interplay of somatic alterations and immune infiltration modulates response to PD-1 blockade in advanced clear cell renal cell carcinoma. Nat Med 2020; 26: 909-918.
[22] TGF-β attenuates tumor response to PD-L1 blockade by contributing to exclusion of T cells (gene.com) (http://research-pub.gene.com/IMvigor210CoreBiologies/).
[23] Zhao Y and Adjei AA. Targeting angiogenesis in cancer therapy: moving beyond vascular endothelial growth factor. Oncologist 2015; 20: 660-73.
[24] Normanno N, Bianco C, De Luca A and Salomon DS. The role of EGF-related peptides in tumor growth. Front Biosci 2001; 6: D685-707.
[25] Hynes NE and Lane HA. ERBB receptors and cancer: the complexity of targeted inhibitors. Nat Rev Cancer 2005; 5: 341-54.
[26] Wang Y, Jing Y, Ding L, Zhang X, Song Y, Chen S, Zhao X, Huang X, Pu Y, Wang Z, Ni Y and Hu Q. Epiregulin reprograms cancer-associated fibroblasts and facilitates oral squamous cell carcinoma invasion via JAK2-STAT3 pathway. J Exp Clin Cancer Res 2019; 38: 274.
[27] Yun J, Song SH, Park J, Kim HP, Yoon YK, Lee KH, Han SW, Oh DY, Im SA, Bang YJ and Kim TY. Gene silencing of EREG mediated by DNA methylation and histone modification in human gastric cancers. Lab Invest 2012; 92: 1033-1044.
[28] Byeon SJ, Lee HS, Kim MA, Lee BL and Kim WH. Expression of the ERBB family of ligands and receptors in gastric cancer. Pathobiology 2017; 84: 210-217.
[29] Suematsu H, Hashimoto I, Hiroshima Y, Watanabe H, Kano K, Takahashi K, Aoyama T, Yamada T, Tamagawa H, Ogata T, Yukawa N, Rino Y, Masuda M, Miyagi Y and Oshima T. Clinical significance of EREG gene expression in gastric cancer tissue after curative surgery. Anticancer Res 2022; 42: 3873-3878.
[30] Bièche I, Lerebours F, Tozlu S, Espie M, Marty M and Lidereau R. Molecular profiling of inflammatory breast cancer: identification of a

poor-prognosis gene expression signature. Clin Cancer Res 2004; 10: 6789-6795.
[31] Xia Q, Zhou Y, Yong H, Wang X, Zhao W, Ding G, Zhu J, Li X, Feng Z and Wang B. Elevated epiregulin expression predicts poor prognosis in gastric cancer. Pathol Res Pract 2019; 215: 873-879.
[32] Xie Y, Xie F, Zhang L, Zhou X, Huang J, Wang F, Jin J, Zhang L, Zeng L and Zhou F. Targeted anti-tumor immunotherapy using tumor infiltrating cells. Adv Sci (Weinh) 2021; 8: e2101672.
[33] Blattman JN and Greenberg PD. Cancer immunotherapy: a treatment for the masses. Science 2004; 305: 200-205.
[34] Hu X, Zhang J, Wang J, Fu J, Li T, Zheng X, Wang B, Gu S, Jiang P, Fan J, Ying X, Zhang J, Carroll MC, Wucherpfennig KW, Hacohen N, Zhang F, Zhang P, Liu JS, Li B and Liu XS. Landscape of B cell immunity and related immune evasion in human cancers. Nat Genet 2019; 51: 560-567.
[35] Helmink BA, Reddy SM, Gao J, Zhang S, Basar R, Thakur R, Yizhak K, Sade-Feldman M, Blando J, Han G, Gopalakrishnan V, Xi Y, Zhao H, Amaria RN, Tawbi HA, Cogdill AP, Liu W, LeBleu VS, Kugeratski FG, Patel S, Davies MA, Hwu P, Lee JE, Gershenwald JE, Lucci A, Arora R, Woodman S, Keung EZ, Gaudreau PO, Reuben A, Spencer CN, Burton EM, Haydu LE, Lazar AJ, Zapassodi R, Hudgens CW, Ledesma DA, Ong S, Bailey M, Warren S, Rao D, Krijgsman O, Rozeman EA, Peeper D, Blank CU, Schumacher TN, Butterfield LH, Zelazowska MA, McBride KM, Kalluri R, Allison J, Petitprez F, Fridman WH, Sautès-Fridman C, Hacohen N, Rezvani K, Sharma P, Tetzlaff MT, Wang L and Wargo JA. B cells and tertiary lymphoid structures promote immunotherapy response. Nature 2020; 577: 549-555.
[36] Shoari A, Tahmasebi M, Khodabakhsh F, Cohan RA, Oghalaie A and Behdani M. Angiogenic biomolecules specific nanobodies application in cancer imaging and therapy; review and updates. Int Immunopharmacol 2022; 105: 108585.
[37] Geindreau M, Ghiringhelli F and Bruchard M. Vascular endothelial growth factor, a key modulator of the anti-tumor immune response. Int J Mol Sci 2021; 22: 4871.
[38] Jászai J and Schmidt MHH. Trends and challenges in tumor anti-angiogenic therapies. Cells 2019; 8: 1102.
[39] Baker JB, Dutta D, Watson D, Maddala T, Munneke BM, Shak S, Rowinsky EK, Xu LA, Harbison CT, Clark EA, Mauro DJ and Khambata-Ford S. Tumour gene expression predicts response to cetuximab in patients with KRAS wild-type metastatic colorectal cancer. Br J Cancer 2011; 104: 488-95.
[40] Ducreux M, Chamseddine A, Laurent-Puig P, Smolenschi C, Hollebecque A, Dartigues P, Samallin E, Boige V, Malka D and Gelli M. Molecular targeted therapy of BRAF-mutant colorectal cancer. Ther Adv Med Oncol 2019; 11: 1758835919856494.
[41] Santin AD, Sill MW, McMeekin DS, Leitao MM Jr, Brown J, Sutton GP, Van Le L, Griffin P and Boardman CH. Phase II trial of cetuximab in the treatment of persistent or recurrent squamous or non-squamous cell carcinoma of the cervix: a Gynecologic Oncology Group Study. Gynecol Oncol 2011; 122: 495-500.
[42] Kurtz JE, Hardy-Bessard AC, Deslandres M, Lavau-Denes S, Largillier R, Roemer-Becuwe C, Weber B, Guillemet C, Paraiso D and Pujade-Lauraine E. Cetuximab, topotecan and cisplatin for the treatment of advanced cervical cancer: a phase II GINECO trial. Gynecol Oncol 2009; 113: 16-20.
[43] Farley J, Sill MW, Birrer M, Walker J, Schilder RJ, Thigpen JT, Coleman RL, Miller BE, Rose PG and Lankes HA. Phase II study of cisplatin plus cetuximab in advanced, recurrent, and previously treated cancers of the cervix and evaluation of epidermal growth factor receptor immunohistochemical expression: a Gynecologic Oncology Group Study. Gynecol Oncol 2011; 121: 303-8.
[44] Pignata S, Scambia G, Lorusso D, De Giorgi U, Nicoletto MO, Lauria R, Mosconi AM, Sacco C, Omarini C, Tagliaferri P, Ferrandina G, Cinieri S, Savarese A, Valabrega G, Pisano C, Salutari V, Raspagliesi F, Kopf B, Cecere SC, Amadio G, Maltese G, Di Napoli M, Greggi S, Signoriello S, Daniele G, Sacco A, Losito S, Normanno N, Perrone F, Gallo C and Piccirillo MC; MITO Investigators. The MITO CERV-2 trial: a randomized phase II study of cetuximab plus carboplatin and paclitaxel, in advanced or recurrent cervical cancer. Gynecol Oncol 2019; 153: 535-540.

Table S1. Differentially expressed genes among three GEO datasets

117 up-regulation genes	76 down-regulation genes
CRNN	LAPTM4B
CRISP3	ATP2C1
MAL	IGK
SPINK5	FADS1
ENDOU	KRT7
CLCA4	CCL18
UPK1A	SOX4
SPRR3	IFI6
THSD4	EPCAM
KRT4	UCP2
EDN3	RRM2
CRCT1	MCM7
ALOX12	ADAM8
KRT1	WHSC1
PPP1R3C	FANCI
GREB1	RARRES1
SLURP1	CEL
BBOX1	NCAPH
KLK12	DSG2
KRT13	ASPM
RHCG	RPL39L
ZBED2	CXCL1
KLK11	APOE
HPGD	PLOD2
SOSTDC1	NEFH
ALOX15B	PLSCR1
IVL	TYMS
NSG1	WARS
TMPRSS11E	NUP210
GPX3	MCM5
ESR1	ISG20
AR	LYN
IL1R2	GABBR1
SCEL	SYT17
CYP3A5	CENPN
DSG1	TOP2A
PRSS3	AURKA
CWH43	RIBC2
ALOX12B	CXCL13
CRABP2	HELLS
CRYAB	CDC45
TMPRSS11D	GINS1
SPRR1A	STAT1
HOPX	FN1
CXCL14	ISG15
GYS2	TRIO
KRT2	MARCKSL1

DSC2
EREG
C2orf54
SPRR1B
EMP1
CDA
KLK10
CXCR2
MALL
AKR1B10
TP53AIP1
DPP4
IL18
SERPINB1
PRSS3P2
PRSS2
HSPB8
PTK6
GLTP
CFD
LOR
TTC39A
KLK7
PI3
SPRR2B
PITX1
PDGFD
OLFM4
SLC24A3
KRT15
KLF4
C1orf116
SPRR2C
FGFBP1
SPON1
ZSCAN18
S100A9
EPB41L3
TP53I3
PAMR1
KCNK7
ZNF91
LYPD3
SLC16A7
MPZL2
LGALS7B
TST
SERPINB2
CD24
CCND1

CDK1
CEP55
GINS2
MYBL2
MCM2
KRT17
NEK2
ECT2
MELK
ENO2
MMP1
WDHD1
DTL
KNTC1
CDKN2A
FOXM1
FOXD1
RFC4
MLF1
APOC1
INHBA
SPP1
CXCL8
SYNGR3
HOXC6
IFI44L
AIM2
MMP12
SYCP2

NOD2
ID4
GSTA4
FGFR2
OCA2
KRT6B
CALML3
ABCA8
NEBL
NMU
SPINK2
PDLIM2
RRAGD
UPP1
FLRT2
VSNL1
AREG
ISL1
CEACAM1
CLDN8

Table S2. The association of significant up-regulated genes with prognosis in CC

Gene	*p* value
CXCL8	6.91E-05
MCM2	0.001230012
EREG	0.002578166
CXCL1	0.004764673
MCM5	0.004809738
SYNGR3	0.005721543
RIBC2	0.00617651
MMP1	0.009270152
SYCP2	0.010203898
GPX3	0.010494776
TP53I3	0.011402958
TYMS	0.014361662
DSG2	0.016688614
SPP1	0.017680766
INHBA	0.019860844
GINS2	0.027273954
HOPX	0.027653721
PLOD2	0.030715537
FGFR2	0.038394338
SPON1	0.039650047
UCP2	0.042142338
GLTP	0.043464967
AR	0.045663856
CALML3	0.047188121
LOR	0.047808666

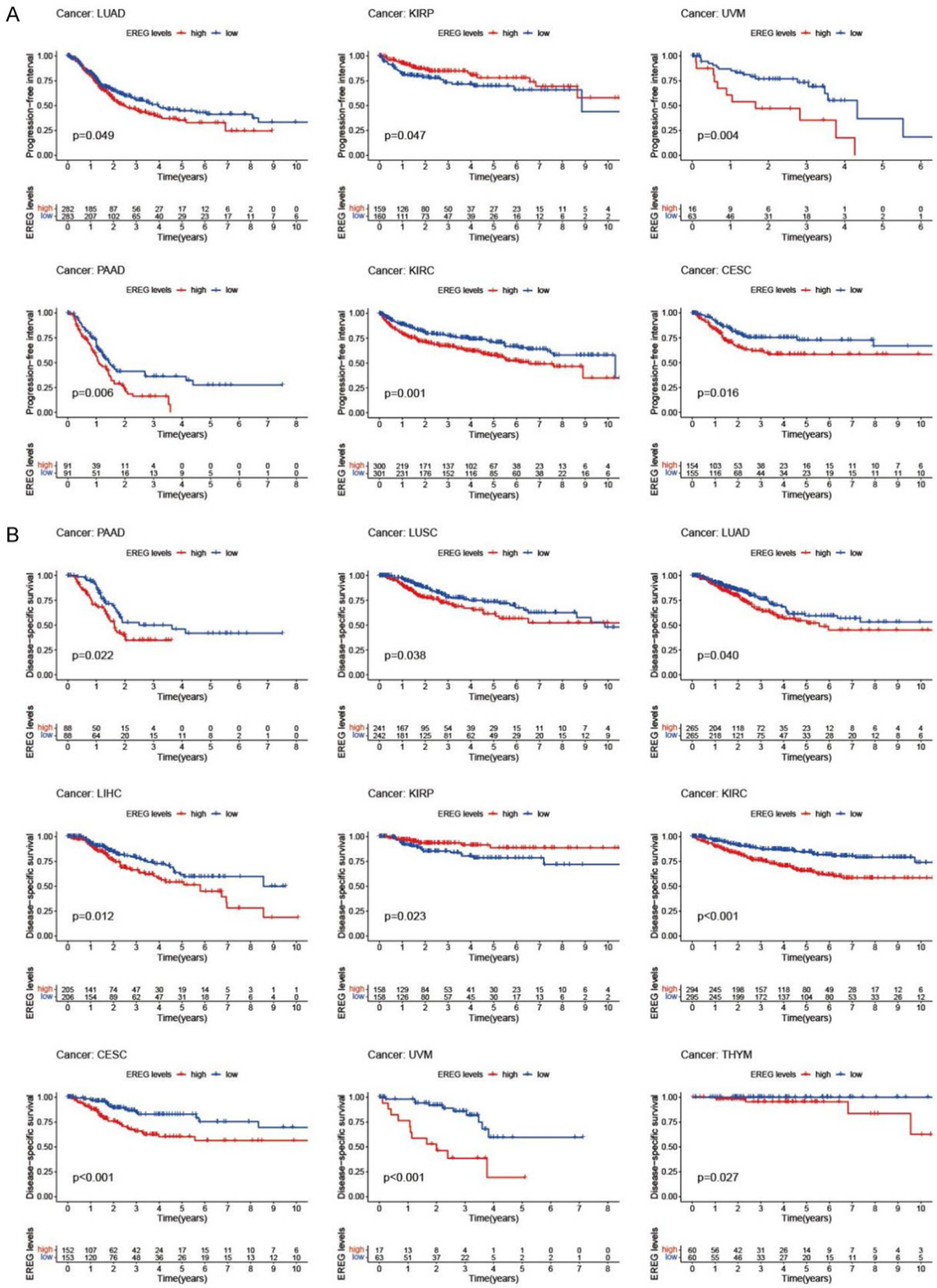

Figure S1. KM curves of high and low EREG expression with DSS (A) and PFI (B).

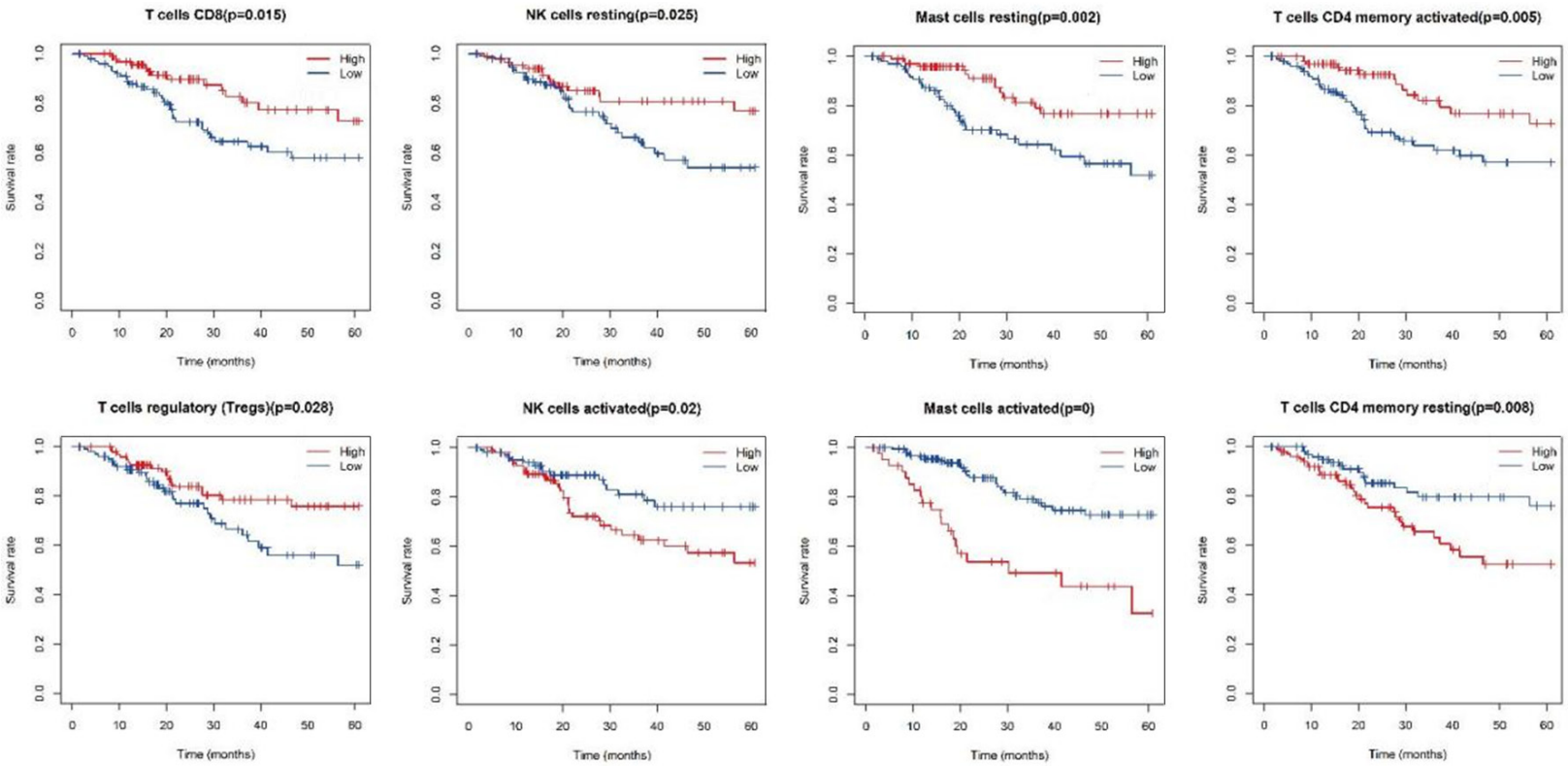

Figure S2. KM curves of high and low immune cells infiltration level with prognosis in CC.

EREG expression with cervical cancer prognosis

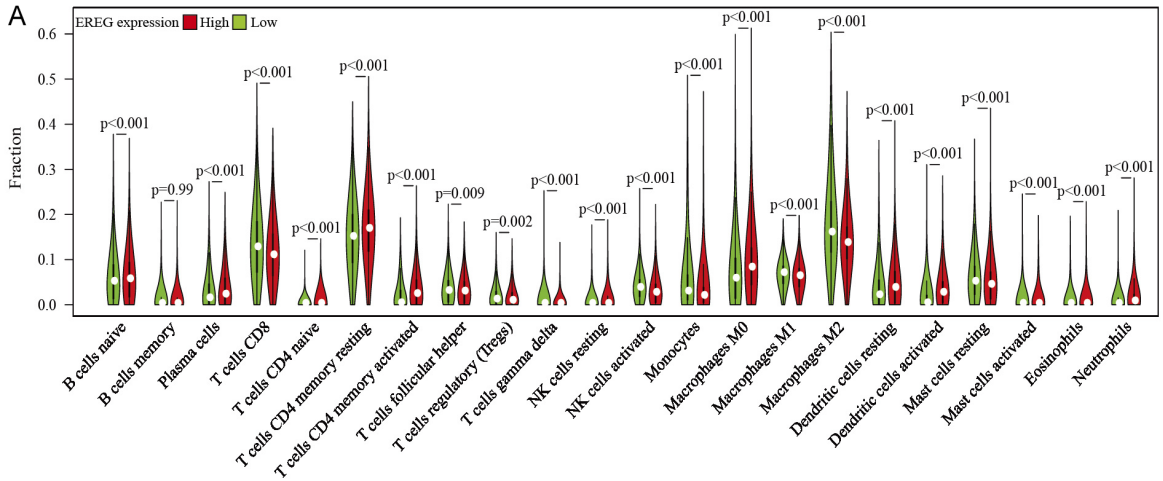

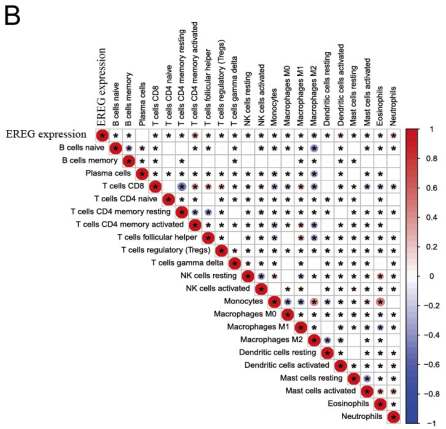

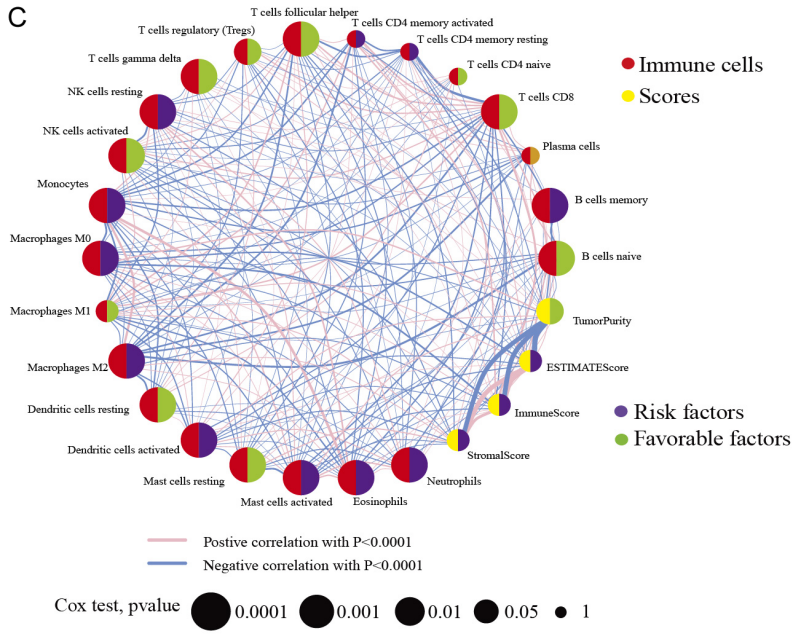

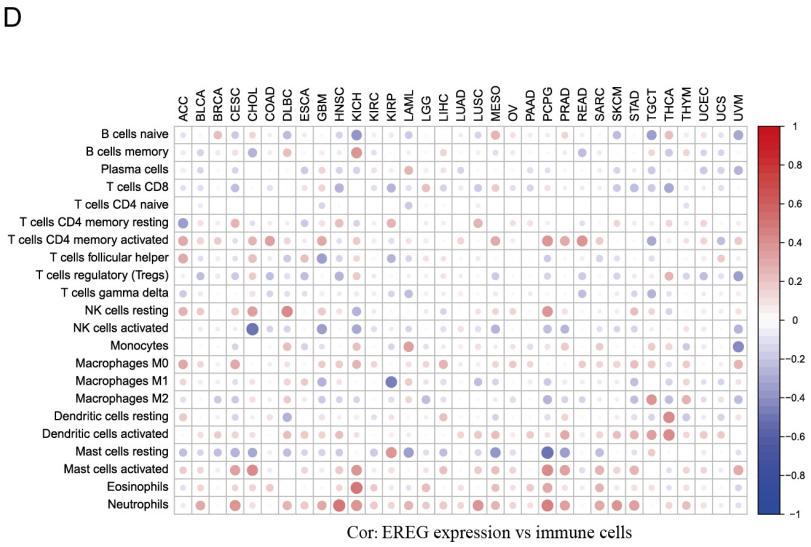

E

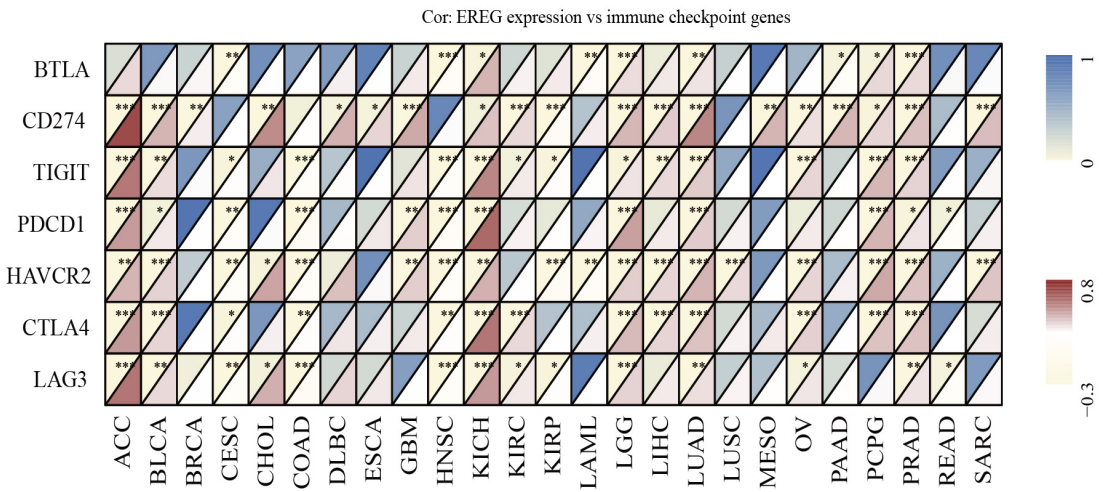

Figure S3. The infiltration difference of immune cells between high- and low EREG expression in 33 tumor types (A); Cellular interaction of immune cells with EREG in TME in pan-cancer analysis (B); Cellular interaction of immune cells with prognosis in pan-cancer analysis (C); The correlation of EREG expression and immune cells in 33 tumor types (D); The correlation of EREG expression and immune checkpoint genes in 33 tumor types (E). (*P < 0.05; **P < 0.01; ***P < 0.001).

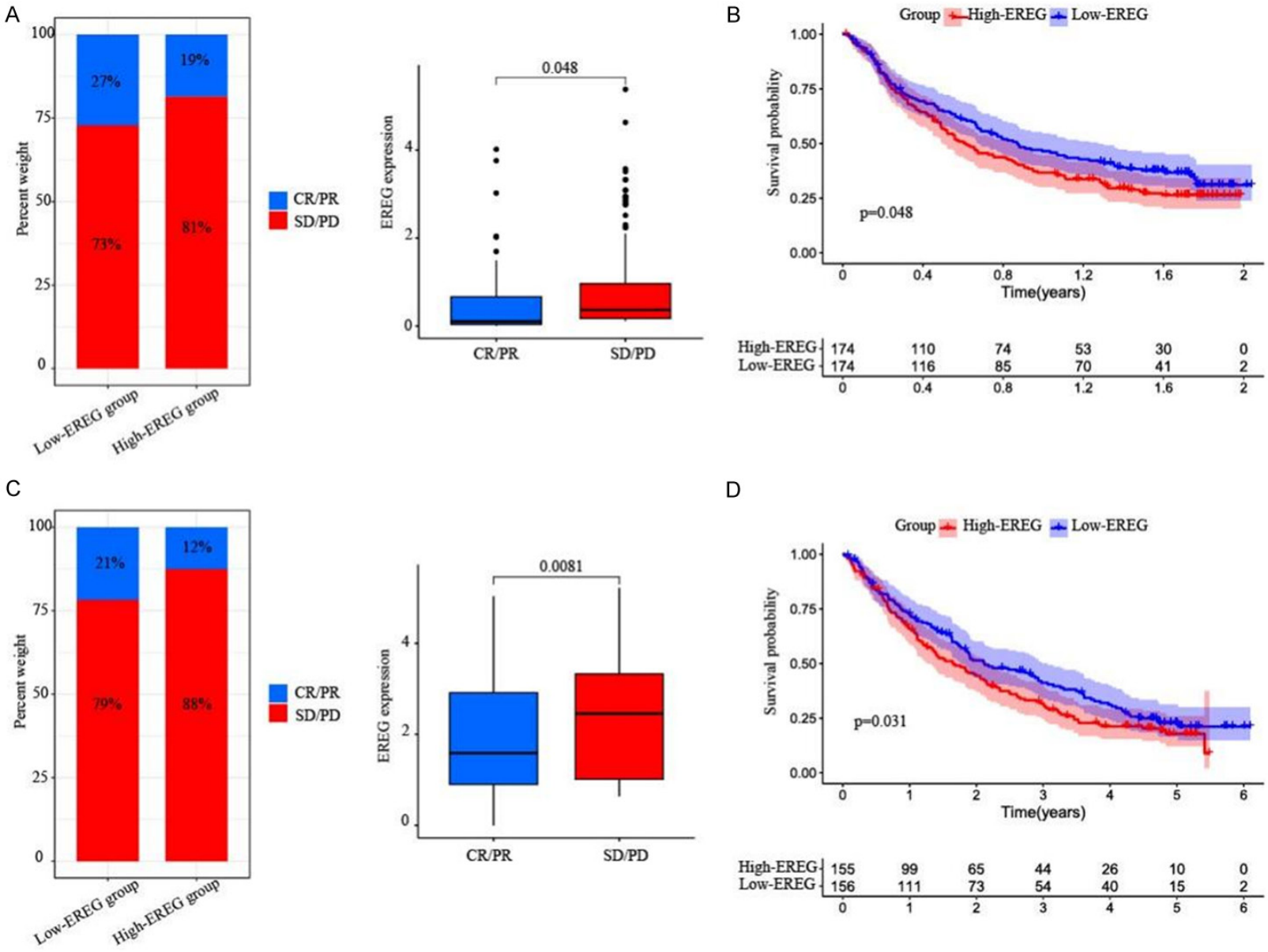

Figure S4. Differences in response rate of CR/PR between high and low EREG group in the cohort of Braun et al (A); Survival analysis showing the prognosis of patients receiving immunotherapy between high and low LMS group in the cohort of Braun et al (B); Differences in response rate of CR/PR between high and low EREG group in the cohort of IMvigor210 (C); Survival analysis showing the prognosis of patients receiving immunotherapy between high and low EREG group in the cohort of IMvigor210 (D).

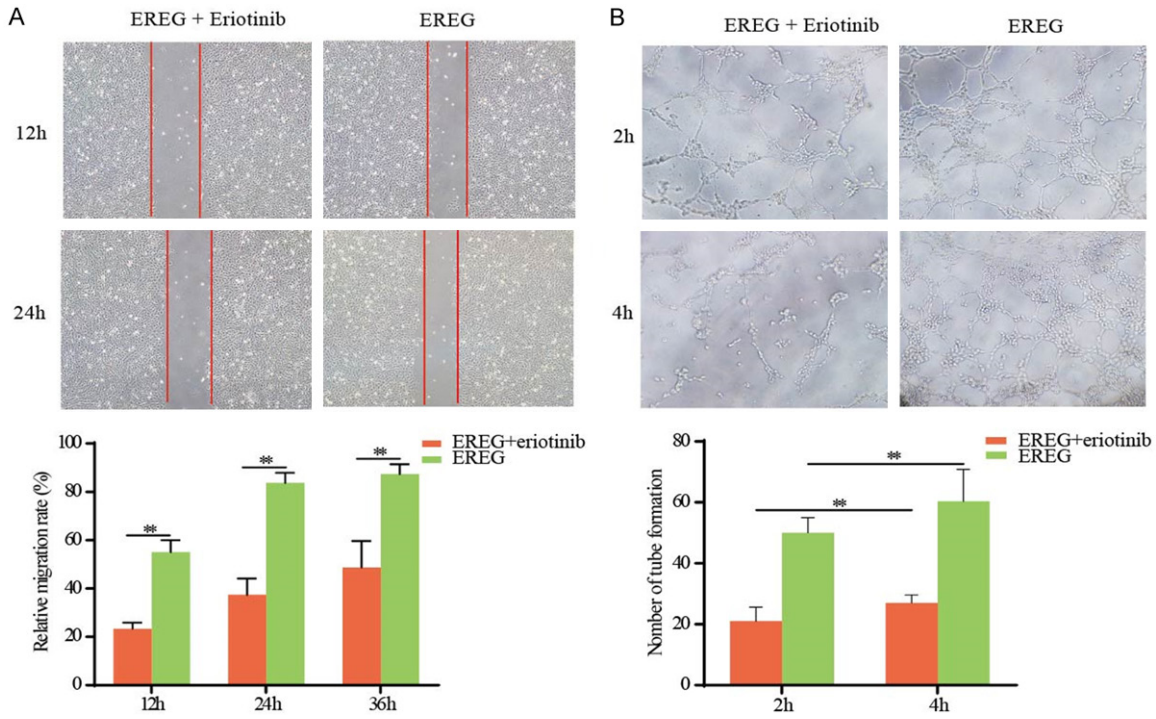

Figure S5. Scratch test showing that eriotinib attenuates the effect of EREG on ECs migration (A); Tube formation test showing that eriotinib attenuates the effect of EREG on ECs tubule forming ability (B). (*P < 0.05; **P < 0.01; ***P < 0.001).